



# Fabrication and microwave absorbing properties of Ni–Zn spinel ferrites

Dong-Lin Zhao\*, Qiang Lv, Zeng-Min Shen

State Key Laboratory of Chemical Resource Engineering, Beijing University of Chemical Technology, Beijing 100029, China

## ARTICLE INFO

### Article history:

Received 23 November 2008  
Received in revised form 29 January 2009  
Accepted 30 January 2009  
Available online 10 February 2009

### Keywords:

Permanent magnets  
Powder metallurgy  
Scanning and transmission electron microscopy  
X-ray diffraction  
Magnetic measurements

## ABSTRACT

Ni–Zn spinel ferrite and Cu-doped, Co-doped Ni–Zn spinel ferrites were prepared by a conventional ceramic processing method. Microwave absorption, complex permittivity and permeability of the  $(\text{Ni}_{0.5}\text{Zn}_{0.5})\text{Fe}_2\text{O}_4$ ,  $(\text{Ni}_{0.4}\text{Cu}_{0.2}\text{Zn}_{0.4})\text{Fe}_2\text{O}_4$  and  $(\text{Ni}_{0.4}\text{Co}_{0.2}\text{Zn}_{0.4})\text{Fe}_2\text{O}_4$  spinel ferrites within the frequency range of 0.5–18 GHz were investigated. The reflection loss calculation results show that the prepared Ni–Zn spinel ferrite and Cu-doped, Co-doped Ni–Zn spinel ferrites are good electromagnetic wave absorbers in the microwave range. The single layer  $(\text{Ni}_{0.4}\text{Co}_{0.2}\text{Zn}_{0.4})\text{Fe}_2\text{O}_4$  spinel ferrite absorber with a thickness of 3 mm achieved a reflection loss below  $-10$  dB (90% absorption) at 3.9–11.5 GHz, and the minimum value was  $-17.01$  dB at 6.1 GHz. Compared with the performances of the single layer spinel ferrite absorbers, not only the matching frequencies of the double layer spinel ferrite absorbers were shifted to higher values, but also the microwave absorbing frequency bands were expanded. When the first layer and second layer are  $(\text{Ni}_{0.5}\text{Zn}_{0.5})\text{Fe}_2\text{O}_4$  and  $(\text{Ni}_{0.4}\text{Co}_{0.2}\text{Zn}_{0.4})\text{Fe}_2\text{O}_4$  spinel ferrites, respectively, the laminated double layer spinel ferrite absorber with a thickness of 3 mm achieved a reflection loss below  $-10$  dB at 3.3–12.7 GHz, and the minimum value was  $-49.1$  dB at 11.8 GHz.

© 2009 Elsevier B.V. All rights reserved.

## 1. Introduction

Much attention has been focused on microwave absorbing materials because of the facts that they can absorb energy from microwave and that they can be widely used in the stealth technology of aircrafts, television image interference of high-rise buildings, and microwave dark-room protection, etc. [1–4]. The manufacture of microwave absorbing materials involves the use of compounds capable of generating dielectric and/or magnetic losses when impinged by an electromagnetic wave. Extensive study has been carried out to develop microwave absorbing materials with high efficiency and new absorption materials [1,5–22]. By controlling the material type (dielectric or magnetic) and thickness, loss factor and impedances, and internal optical design, performance of the microwave absorbing material can be optimized for a single narrow band frequency, multiple frequencies, or over a broad frequency spectrum [23].

Spinel ferrites have been utilized as absorbing materials in various forms for many years due to their large magnetic losses and large resistivities. However, in the microwave region, the applications of spinel ferrites are limited at the lower end of microwave

frequency (1–3 GHz) because of their lower natural resonance frequencies in comparison with those of other types of ferrites, such as hexaferrites [24–32]. Within the gigahertz range, the permittivity of a ferrite is almost a constant with its imaginary part close to 0. Therefore, the dielectric loss is almost negligible, and its absorbing performance mainly depends on the magnetic loss. One of the frequently used methods to tune the complex permeability of spinel ferrites is to dope the ferrites with many metallic ions, such as Cu, Zn, Co, Li, Mn, Mg, etc. [33–38]. For this purpose, some attempts were made to verify the correlation between the material constants, permittivity ( $\epsilon_r = \epsilon' - j\epsilon''$ ) and permeability ( $\mu_r = \mu' - j\mu''$ ) and the microwave absorption in the sintered ferrites that contain divalent metal ions [1,33–44].

In order to further exploit the potentials of spinel ferrites in microwave absorbing applications, in our present work, we investigated the fabrication process of Ni–Zn spinel ferrite and Cu-doped, Co-doped Ni–Zn spinel ferrites and their microwave absorbing properties, and the possible microwave absorbing mechanisms were discussed.

## 2. Experimental

Ni–Zn spinel ferrite and Cu-doped, Co-doped Ni–Zn spinel ferrites were fabricated by a conventional ceramic processing method. The mixtures of  $\text{Fe}_2\text{O}_3$ , NiO, ZnO, CuO and  $\text{Co}_2\text{O}_3$  were sintered at 1250 °C for 2 h. The compositions of Ni–Zn spinel ferrites were tuned by changing the amounts of CuO and  $\text{Co}_2\text{O}_3$  in the mixtures. The particle size of prepared ferrite powders was controlled by passing the grinded

\* Corresponding author. Tel.: +86 10 64434914; fax: +86 10 64454912.  
E-mail address: [dlzhao@mail.buct.edu.cn](mailto:dlzhao@mail.buct.edu.cn) (D.-L. Zhao).

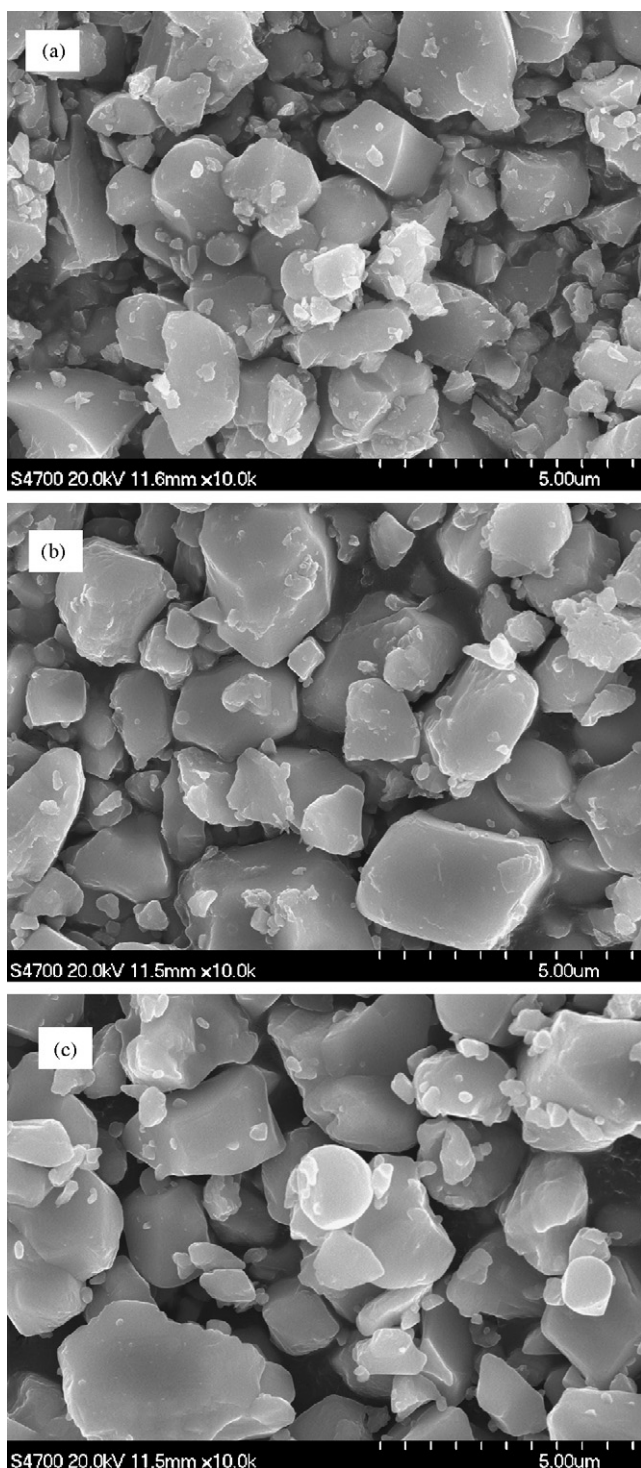


**Fig. 1.** SEM images of  $(\text{Ni}_{0.5}\text{Zn}_{0.5})\text{Fe}_2\text{O}_4$  (a),  $(\text{Ni}_{0.4}\text{Cu}_{0.2}\text{Zn}_{0.4})\text{Fe}_2\text{O}_4$  (b) and  $(\text{Ni}_{0.4}\text{Co}_{0.2}\text{Zn}_{0.4})\text{Fe}_2\text{O}_4$  (c) spinel ferrites.

powders through a sieve with an average aperture size of 74  $\mu\text{m}$ . The morphology and microstructure of the Ni–Zn spinel ferrite and Cu-doped, Co-doped Ni–Zn spinel ferrites were observed using a field-emission scanning electron microscopy (FESEM, Hitachi S-4700). Their phases and crystalline microstructures were characterized by X-ray diffraction (XRD), which was carried out in a Rigaku D/MAX-3CX diffractometer using the  $\text{K}\alpha$  line of Cu as a radiation source. The compositions of Ni–Zn spinel ferrite and Cu-doped, Co-doped Ni–Zn spinel ferrites were measured by the energy dispersive X-ray (EDX) technique. To measure the microwave electromagnetic properties (complex permeability and complex permittivity) on a HP8722ES vector network analyzer, each sample was prepared by mixing the spinel ferrite powders with paraffin homogeneously and was pressed into a ring shape. The inner

and outer diameters of ring samples are 3 and 7 mm, respectively. The weight ratio of ferrite/paraffin was kept as a constant as 6:1 for each sample. The frequency range selected for the electromagnetic measurements was 0.5–18 GHz. Based on the measured complex permittivity and permeability, we assumed that a single layer of ferrites/paraffin composites was attached on a metal plate. Then, the microwave absorbing performances were evaluated by the following equation [33]:

$$\text{RL} = 20 \log \left| \frac{Z_{\text{in}} - Z_0}{Z_{\text{in}} + Z_0} \right| \quad (1)$$

where RL denotes the reflection loss in dB unit.  $Z_0$  is the characteristic impedance of free space.  $Z_{\text{in}}$  is the input characteristic impedance at the absorber/free space interface, which can be expressed as

$$Z_{\text{in}} = Z_0 \sqrt{\frac{\mu_r}{\epsilon_r}} \tanh \left( j \left( \frac{2\pi ft}{c} \right) \sqrt{\mu_r \epsilon_r} \right) \quad (2)$$

where  $c$  is the velocity of light,  $t$  is the thickness of a ferrite absorber. In this paper, all  $t$  values are in mm unit.  $\epsilon_r$  and  $\mu_r$  are the measured relative complex permeability and permittivity, respectively.

### 3. Results and discussion

Ni–Zn spinel ferrite and Cu-doped, Co-doped Ni–Zn spinel ferrites were prepared by a conventional ceramic processing method. Fig. 1 shows the SEM micrographs of  $(\text{Ni}_{0.5}\text{Zn}_{0.5})\text{Fe}_2\text{O}_4$ ,  $(\text{Ni}_{0.4}\text{Cu}_{0.2}\text{Zn}_{0.4})\text{Fe}_2\text{O}_4$  and  $(\text{Ni}_{0.4}\text{Co}_{0.2}\text{Zn}_{0.4})\text{Fe}_2\text{O}_4$  ferrites. The powders are almost spherical with diameters ranging from 0.2 to 4  $\mu\text{m}$ . These powders are polydisperse and some of them agglomerated due to magneto-dipole interactions between powders.

Fig. 2 shows the XRD patterns of the  $(\text{Ni}_{0.5}\text{Zn}_{0.5})\text{Fe}_2\text{O}_4$  spinel ferrite as well as the  $(\text{Ni}_{0.4}\text{Cu}_{0.2}\text{Zn}_{0.4})\text{Fe}_2\text{O}_4$  and  $(\text{Ni}_{0.4}\text{Co}_{0.2}\text{Zn}_{0.4})\text{Fe}_2\text{O}_4$  spinel ferrites. The main peaks of the prepared samples are at  $2\theta = 18.31^\circ$ ,  $30.11^\circ$ ,  $35.45^\circ$ ,  $37.08^\circ$ ,  $43.08^\circ$ ,  $53.44^\circ$ ,  $56.96^\circ$ ,  $62.54^\circ$ ,  $70.97^\circ$ ,  $73.99^\circ$ ,  $74.98^\circ$ ,  $78.96^\circ$ ,  $86.74^\circ$  and  $89.64^\circ$ , which exhibit typical spinel structure (space group  $Fd\bar{3}m$ ). No other phases have been detected.

Saturation magnetization  $M_s$ , remanent magnetization  $M_r$  and coercivity  $H_c$  are the main technical parameters to characterize the magnetism of a ferromagnetic particle sample. The hysteresis loops of  $(\text{Ni}_{0.5}\text{Zn}_{0.5})\text{Fe}_2\text{O}_4$ ,  $(\text{Ni}_{0.4}\text{Cu}_{0.2}\text{Zn}_{0.4})\text{Fe}_2\text{O}_4$  and  $(\text{Ni}_{0.4}\text{Co}_{0.2}\text{Zn}_{0.4})\text{Fe}_2\text{O}_4$  spinel ferrites are shown in Fig. 3.  $M_s$  and  $H_c$  are  $83.48 \text{ emu g}^{-1}$  and 24 Oe for the  $(\text{Ni}_{0.5}\text{Zn}_{0.5})\text{Fe}_2\text{O}_4$  ferrite, and  $62.18 \text{ emu g}^{-1}$  and 10 Oe for the  $(\text{Ni}_{0.4}\text{Cu}_{0.2}\text{Zn}_{0.4})\text{Fe}_2\text{O}_4$  ferrite, and  $88.91 \text{ emu g}^{-1}$  and 53 Oe for the  $(\text{Ni}_{0.4}\text{Co}_{0.2}\text{Zn}_{0.4})\text{Fe}_2\text{O}_4$  ferrite, respectively.

In order to investigate the intrinsic reasons for microwave absorption of the  $(\text{Ni}_{0.5}\text{Zn}_{0.5})\text{Fe}_2\text{O}_4$ ,  $(\text{Ni}_{0.4}\text{Cu}_{0.2}\text{Zn}_{0.4})\text{Fe}_2\text{O}_4$  and  $(\text{Ni}_{0.4}\text{Co}_{0.2}\text{Zn}_{0.4})\text{Fe}_2\text{O}_4$  spinel ferrites, the complex permittivities and permeabilities of the ferrite/paraffin composites were measured by the coaxial line method. The real parts ( $\mu'$ ) and imaginary

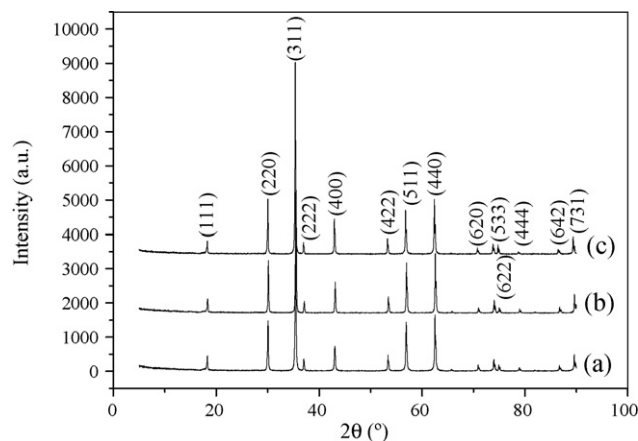


**Fig. 2.** XRD patterns of  $(\text{Ni}_{0.5}\text{Zn}_{0.5})\text{Fe}_2\text{O}_4$  (a),  $(\text{Ni}_{0.4}\text{Cu}_{0.2}\text{Zn}_{0.4})\text{Fe}_2\text{O}_4$  (b) and  $(\text{Ni}_{0.4}\text{Co}_{0.2}\text{Zn}_{0.4})\text{Fe}_2\text{O}_4$  (c) spinel ferrites.

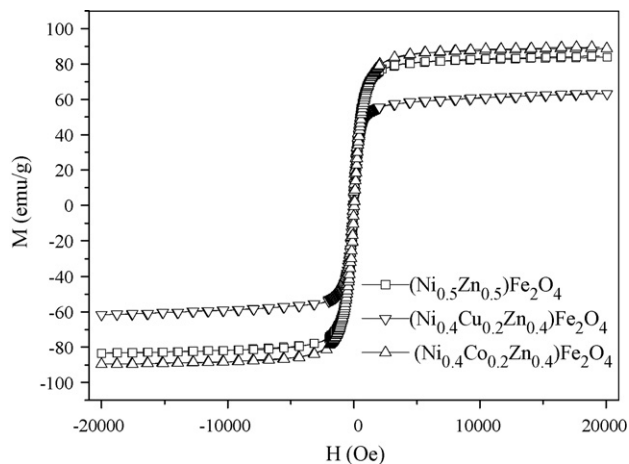


Fig. 3. Hysteresis loops of  $(\text{Ni}_{0.5}\text{Zn}_{0.5})\text{Fe}_2\text{O}_4$ ,  $(\text{Ni}_{0.4}\text{Cu}_{0.2}\text{Zn}_{0.4})\text{Fe}_2\text{O}_4$  and  $(\text{Ni}_{0.4}\text{Co}_{0.2}\text{Zn}_{0.4})\text{Fe}_2\text{O}_4$  spinel ferrites.

parts ( $\mu''$ ) of the complex permeabilities of the  $(\text{Ni}_{0.5}\text{Zn}_{0.5})\text{Fe}_2\text{O}_4$ ,  $(\text{Ni}_{0.4}\text{Cu}_{0.2}\text{Zn}_{0.4})\text{Fe}_2\text{O}_4$  and  $(\text{Ni}_{0.4}\text{Co}_{0.2}\text{Zn}_{0.4})\text{Fe}_2\text{O}_4$  ferrites are shown in Fig. 4. The  $\mu'$  values of the Ni–Zn spinel ferrites in the frequency range of 0.5–1.5 GHz decrease after doped with Cu and Co. In the rest frequency range, such a clear dependence does not

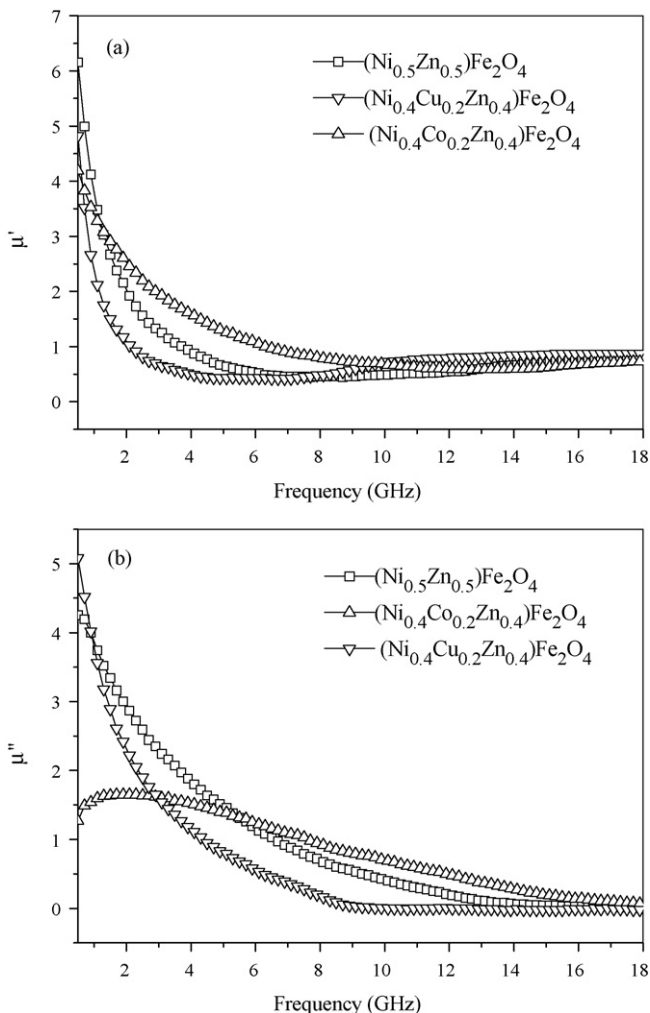


Fig. 4. Frequency dependence of  $\mu'$  (a) and  $\mu''$  (b) of the  $(\text{Ni}_{0.5}\text{Zn}_{0.5})\text{Fe}_2\text{O}_4/\text{paraffin}$ ,  $(\text{Ni}_{0.4}\text{Cu}_{0.2}\text{Zn}_{0.4})\text{Fe}_2\text{O}_4/\text{paraffin}$  and  $(\text{Ni}_{0.4}\text{Co}_{0.2}\text{Zn}_{0.4})\text{Fe}_2\text{O}_4/\text{paraffin}$  composites.

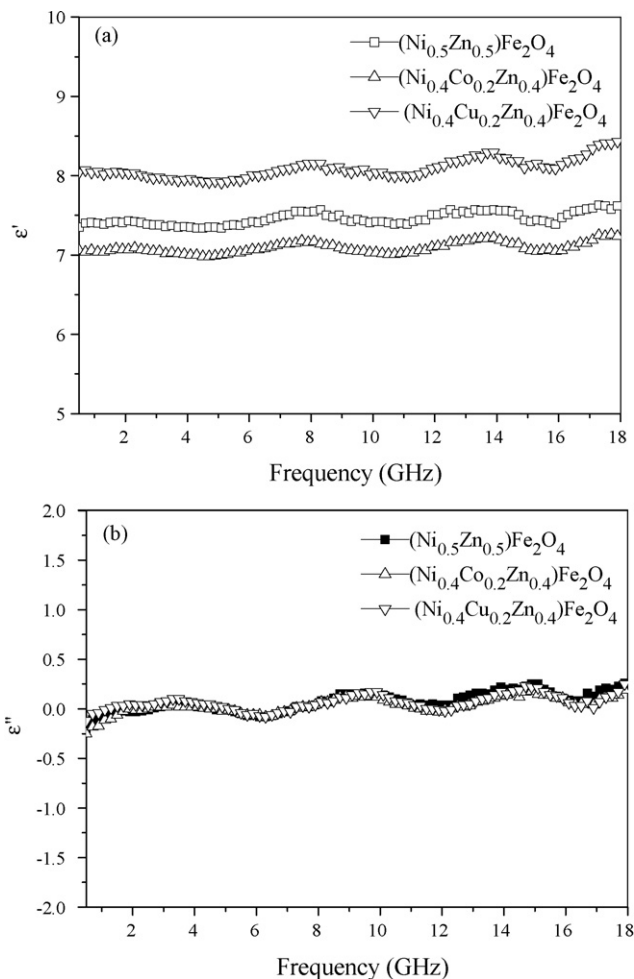
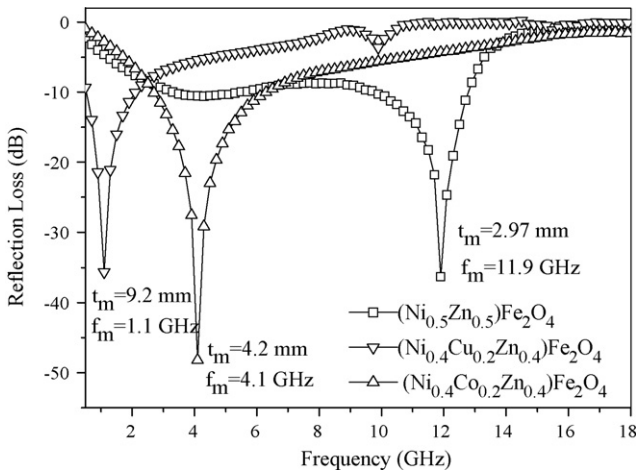


Fig. 5. Frequency dependence of  $\epsilon'$  (a) and  $\epsilon''$  (b) of the  $(\text{Ni}_{0.5}\text{Zn}_{0.5})\text{Fe}_2\text{O}_4/\text{paraffin}$ ,  $(\text{Ni}_{0.4}\text{Cu}_{0.2}\text{Zn}_{0.4})\text{Fe}_2\text{O}_4/\text{paraffin}$  and  $(\text{Ni}_{0.4}\text{Co}_{0.2}\text{Zn}_{0.4})\text{Fe}_2\text{O}_4/\text{paraffin}$  composites.

exist for the  $\mu'$  values. As for the  $\mu''$ -frequency spectra (Fig. 4(b)),  $\mu''$  values of the  $(\text{Ni}_{0.4}\text{Co}_{0.2}\text{Zn}_{0.4})\text{Fe}_2\text{O}_4$  ferrite are bigger than those of the  $(\text{Ni}_{0.5}\text{Zn}_{0.5})\text{Fe}_2\text{O}_4$  and  $(\text{Ni}_{0.4}\text{Cu}_{0.2}\text{Zn}_{0.4})\text{Fe}_2\text{O}_4$  ferrites in the frequency range of 5.5–18 GHz. The real parts ( $\epsilon'$ ) and imaginary parts ( $\epsilon''$ ) of the complex permittivities of Ni–Zn spinel ferrites are shown in Fig. 5. The  $\epsilon'$  values of the Ni–Zn spinel ferrite are bigger than those of the Co-doped Ni–Zn spinel ferrite, but smaller than those of the Cu-doped Ni–Zn ferrite. The  $\epsilon''$  curves of these samples are very similar and the  $\epsilon''$  values are around 0. Therefore, the microwave absorptions of the Ni–Zn spinel ferrite and Cu-doped, Co-doped Ni–Zn spinel ferrites result mainly from magnetic loss rather than dielectric loss. According to the ordinary permittivity dispersion spectra for polycrystalline ferrites in GHz range, there are two mechanisms responsible for the permittivity dispersion: electron polarization and ion polarization. The  $\epsilon'$  values are usually found invariable with frequency, and the  $\epsilon''$  values are found very close to zero [45]. Therefore, the dielectric losses for all prepared samples are almost equal to zero. Our results in Fig. 5 are consistent with this well-accepted phenomenon. So only the real parts of permittivities affect the impedance-matching conditions of the Ni–Zn spinel ferrite and Cu-doped, Co-doped Ni–Zn spinel ferrites.

To evaluate the microwave absorbing performances, the RL in dB unit can be calculated based on Eqs. (1) and (2). If the RL values of an absorber are less than  $-10$  dB (90% absorption), then we can say that the absorber works very well for the absorbing purposes. In other words, from the impedance-matching point



**Fig. 6.** Reflection loss of the single layer  $(\text{Ni}_{0.5}\text{Zn}_{0.5})\text{Fe}_2\text{O}_4$ ,  $(\text{Ni}_{0.4}\text{Cu}_{0.2}\text{Zn}_{0.4})\text{Fe}_2\text{O}_4$  and  $(\text{Ni}_{0.4}\text{Co}_{0.2}\text{Zn}_{0.4})\text{Fe}_2\text{O}_4$  spinel ferrites and the matching thickness  $t_m$ .

of view, we can say that  $Z_{in}$  and  $Z_0$  approximately match each other. When the impedances match, the matching thickness  $t_m$  can be defined as the thickness associated with the minimum RL value in a RL–frequency curve. Here, the microwave absorbing frequency band (AFB) is defined as the frequency range, in which the RL values are less than  $-10$  dB. The RL spectra of the single layer  $(\text{Ni}_{0.5}\text{Zn}_{0.5})\text{Fe}_2\text{O}_4$ ,  $(\text{Ni}_{0.4}\text{Cu}_{0.2}\text{Zn}_{0.4})\text{Fe}_2\text{O}_4$  and  $(\text{Ni}_{0.4}\text{Co}_{0.2}\text{Zn}_{0.4})\text{Fe}_2\text{O}_4$  spinel ferrites are shown in Fig. 6. Compared with other samples, the  $(\text{Ni}_{0.5}\text{Zn}_{0.5})\text{Fe}_2\text{O}_4$  spinel ferrite has better performances, no matter in terms of the AFB or the matching thickness: its AFB is 5.2 GHz (3.3–5.5 and 9.7–12.7 GHz), while  $t_m$  is 2.97 mm. The RL values of the single layer  $(\text{Ni}_{0.5}\text{Zn}_{0.5})\text{Fe}_2\text{O}_4$ ,  $(\text{Ni}_{0.4}\text{Cu}_{0.2}\text{Zn}_{0.4})\text{Fe}_2\text{O}_4$  and  $(\text{Ni}_{0.4}\text{Co}_{0.2}\text{Zn}_{0.4})\text{Fe}_2\text{O}_4$  spinel ferrite absorbers with the same thickness of 3 mm are calculated and compared in Fig. 7. Under this circumstance, in terms of the RL values, the  $(\text{Ni}_{0.4}\text{Co}_{0.2}\text{Zn}_{0.4})\text{Fe}_2\text{O}_4$  ferrite has better microwave absorbing performance. The single layer  $(\text{Ni}_{0.4}\text{Co}_{0.2}\text{Zn}_{0.4})\text{Fe}_2\text{O}_4$  ferrite absorber with a thickness of 3 mm achieved a reflection loss below  $-10$  dB (90% absorption) at 3.9–11.5 GHz, and the minimum value was  $-17.01$  dB at 6.1 GHz.

An easier way to tune the microwave absorbing performances is to laminate an absorber with different spinel ferrite layers. In each layer, the ferrite has different complex permeability and complex permittivity values. We laminated an absorber with two layers of

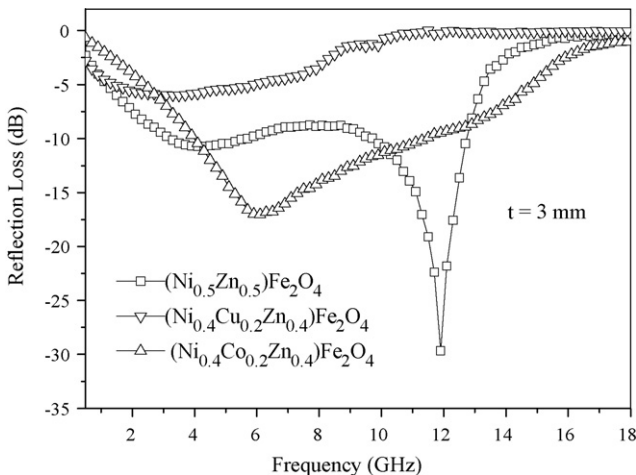


**Fig. 7.** Reflection loss of the single layer  $(\text{Ni}_{0.5}\text{Zn}_{0.5})\text{Fe}_2\text{O}_4$ ,  $(\text{Ni}_{0.4}\text{Cu}_{0.2}\text{Zn}_{0.4})\text{Fe}_2\text{O}_4$  and  $(\text{Ni}_{0.4}\text{Co}_{0.2}\text{Zn}_{0.4})\text{Fe}_2\text{O}_4$  spinel ferrites with the same thickness of 3 mm.

ferrites. Theoretically, for an absorber with two layers of magnetic materials, the following impedance-matching conditions should be satisfied for the best absorbing performances [46]:

$$Z_{in(2)} = \frac{Z_2 [Z_{in(1)} + Z_2 \tanh(j(2\pi ft/c)\sqrt{\mu_{2r}\epsilon_{2r}})]}{Z_2 + Z_{in(1)} \tanh(j(2\pi ft/c)\sqrt{\mu_{2r}\epsilon_{2r}})} = Z_0 \quad (3)$$

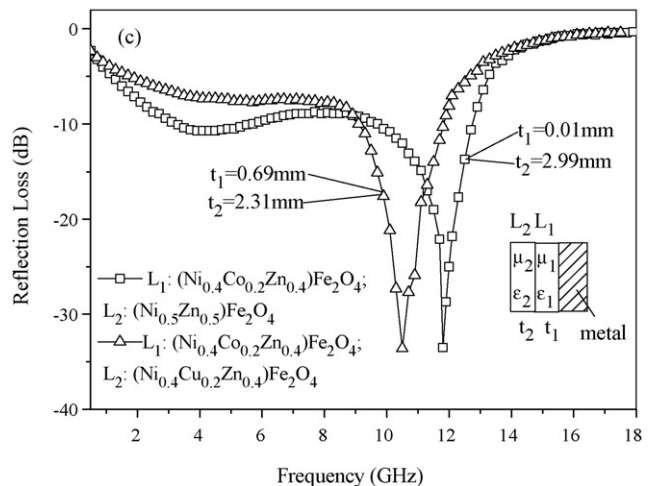
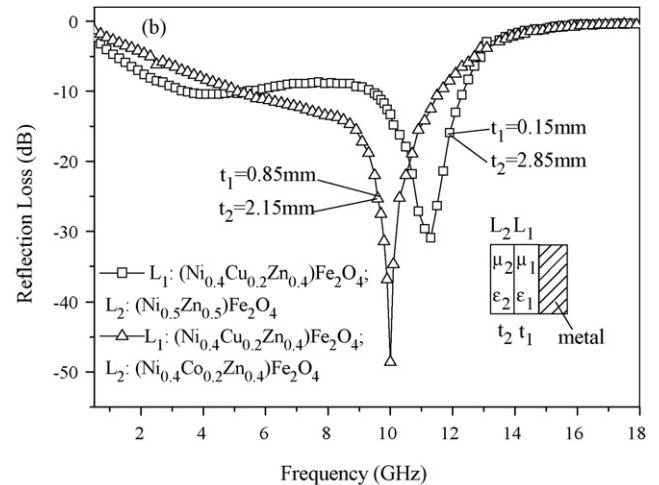
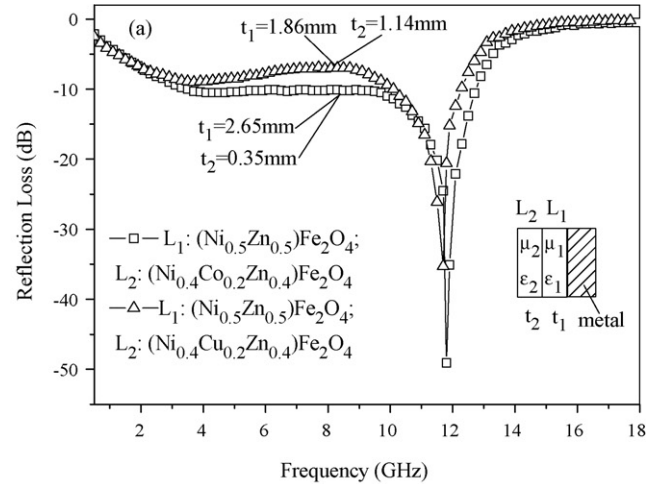


**Fig. 8.** Reflection loss of the laminated absorbers with double ferrite layers with the same thickness of 3 mm ( $t_1$  and  $t_2$  are the thicknesses of ferrites, the inset shows the sequence of ferrites).

where

$$Z_{in(1)} = \sqrt{\frac{\mu_{1r}}{\varepsilon_{1r}}} \tanh \left( j \left( \frac{2\pi ft}{c} \right) \sqrt{\mu_{1r}\varepsilon_{1r}} \right) \quad (4)$$

and

$$Z_2 = \sqrt{\frac{\mu_{2r}}{\varepsilon_{2r}}} \quad (5)$$

$Z_{in(1)}$  is the input impedance at the interface between the first layer ( $L_1$ ) and the second layer ( $L_2$ ).  $Z_{in(2)}$  is the input impedance at the interface between the free space and the outside ferrite layer ( $L_2$ ).

Fig. 8 shows the reflection loss of the laminated absorbers with double spinel ferrite layers with the same thickness of 3 mm. The first layers ( $L_1$ ) are  $(\text{Ni}_{0.5}\text{Zn}_{0.5})\text{Fe}_2\text{O}_4$ ,  $(\text{Ni}_{0.4}\text{Cu}_{0.2}\text{Zn}_{0.4})\text{Fe}_2\text{O}_4$  and  $(\text{Ni}_{0.4}\text{Co}_{0.2}\text{Zn}_{0.4})\text{Fe}_2\text{O}_4$  spinel ferrites in Fig. 8(a–c), respectively. Compared with the performances of the single layer absorber (Figs. 6 and 7), not only the matching frequencies were shifted to higher values, but also the AFBs were expanded. When the first layer ( $L_1$ ) and the second layer ( $L_2$ ) are  $(\text{Ni}_{0.5}\text{Zn}_{0.5})\text{Fe}_2\text{O}_4$  and  $(\text{Ni}_{0.4}\text{Co}_{0.2}\text{Zn}_{0.4})\text{Fe}_2\text{O}_4$  ferrites, respectively, the AFB is 9.4 GHz (3.3–12.7 GHz) and the matching frequency is 11.8 GHz (Fig. 8(a)).

#### 4. Conclusions

Ni–Zn spinel ferrite and Cu-doped, Co-doped Ni–Zn spinel ferrites were prepared by a conventional ceramic processing method. The single layer  $(\text{Ni}_{0.4}\text{Co}_{0.2}\text{Zn}_{0.4})\text{Fe}_2\text{O}_4$  spinel ferrite absorber with a thickness of 3 mm achieved a reflection loss below –10 dB (90% absorption) at 3.9–11.5 GHz, and the minimum value was –17.01 dB at 6.1 GHz. Compared with the performances of the single layer spinel ferrite absorbers, not only the matching frequencies of the double layer spinel ferrite absorbers were shifted to higher values, but also the microwave absorbing frequency bands were expanded. When the first layer and the second layer are  $(\text{Ni}_{0.5}\text{Zn}_{0.5})\text{Fe}_2\text{O}_4$  and  $(\text{Ni}_{0.4}\text{Co}_{0.2}\text{Zn}_{0.4})\text{Fe}_2\text{O}_4$  ferrites, respectively, the laminated double layer spinel ferrite absorber with a thickness of 3 mm achieved a reflection loss below –10 dB at 3.3–12.7 GHz, and the minimum value was –49.1 dB at 11.8 GHz. The reflection loss calculations show that the prepared Ni–Zn spinel ferrite and Cu-doped, Co-doped Ni–Zn spinel ferrites are good electromagnetic wave absorbers in the microwave range.

#### Acknowledgements

This work was supported by the National Natural Science Foundation of China (Grant No. 50672004) and the National High-Tech Research and Development Program (2008AA03Z513).

#### References

[1] C.H. Peng, C.C. Hwang, J. Wan, J.S. Tsai, S.Y. Chen, Mater. Sci. Eng. B 117 (2005) 27–36.

[2] M. Pardavi-Horvath, J. Magn. Magn. Mater. 215–216 (2000) 171–183.  
 [3] J.Y. Shin, J.H. Oh, IEEE Trans. Magn. 29 (1993) 3437–3439.  
 [4] H. Zhu, H.Y. Lin, H.F. Guo, L.F. Yu, Mater. Sci. Eng. B 138 (2007) 101–104.  
 [5] Z.J. Fan, G.H. Luo, Z.F. Zhang, L. Zhou, F. Wei, Mater. Sci. Eng. B 132 (2007) 85–89.  
 [6] S. Ruan, B. Xu, H. Suo, F. Wu, S. Xiang, M. Zhao, J. Magn. Magn. Mater. 212 (2000) 175–177.  
 [7] V.K. Babbar, A. Razdan, R.A. Puri, T.C. Goel, J. Appl. Phys. 87 (2000) 4362–4366.  
 [8] A. Verma, A.K. Saxena, D.C. Dube, J. Magn. Magn. Mater. 263 (2003) 228–234.  
 [9] D.L. Zhao, X. Li, Z.M. Shen, J. Alloys Compd. (2008), doi:10.1016/j.jallcom.2008.03.127.  
 [10] Y. Fan, H. Yang, X. Liu, H. Zhu, G. Zou, J. Alloys Compd. 461 (2008) 490–494.  
 [11] D.L. Zhao, X. Li, Z.M. Shen, Mater. Sci. Eng. B 150 (2008) 105–110.  
 [12] Y. Li, R. Wang, F. Qi, C. Wang, Appl. Surf. Sci. 254 (2008) 4708–4715.  
 [13] X.G. Liu, D.Y. Geng, H. Meng, W.B. Cui, F. Yang, D.J. Kang, Z.D. Zhang, Solid State Commun. 149 (2009) 64–67.  
 [14] K. Lakshmi, H. John, K.T. Mathew, R. Joseph, K.E. George, Acta Mater. 57 (2009) 371–375.  
 [15] Z. Li, W. Zhou, T. Lei, F. Luo, Y. Huang, Q. Cao, J. Alloys Compd. (2008), doi:10.1016/j.jallcom.2008.07.070.  
 [16] D.L. Zhao, Z.M. Shen, Mater. Lett. 62 (2008) 3704–3706.  
 [17] X. Li, X. Han, Y. Tan, P. Xu, J. Alloys Compd. 464 (2008) 352–356.  
 [18] H. Zhao, X. Sun, C. Mao, J. Du, Physica B 404 (2009) 69–72.  
 [19] W. Zhao, Q. Zhang, H. Zhang, J. Zhang, J. Alloys Compd. (2008), doi:10.1016/j.jallcom.2008.05.047.  
 [20] D.L. Zhao, X. Li, Z.M. Shen, Compos. Sci. Technol. 68 (2008) 2902–2908.  
 [21] L. Jing, G. Wang, Y. Duan, Y. Jiang, J. Alloys Compd. (2008), doi:10.1016/j.jallcom.2008.08.038.  
 [22] E.M.A. Jamala, P.A. Joyb, P. Kurianc, M.R. Anantharamana, Mater. Sci. Eng. B 156 (2009) 24–31.  
 [23] R.A. Stonier, SAMPE J. 27 (1991) 9–18.  
 [24] P. Lubitz, F.J. Rachford, J. Appl. Phys. 91 (2002) 7613–7616.  
 [25] Z.W. Li, L. Chen, C.K. Ong, J. Appl. Phys. 94 (2003) 5918–5921.  
 [26] F. Tabatabaie, M.H. Fathi, A. Saatchi, A. Ghasemi, J. Alloys Compd. (2008), doi:10.1016/j.jallcom.2008.02.094.  
 [27] G. Mu, N. Chen, X. Pan, H. Shen, M. Gu, Mater. Lett. 62 (2008) 840–842.  
 [28] A. Ghasemi, A. Morisako, J. Alloys Compd. 456 (2008) 485–491.  
 [29] A. Ghasemi, A. Morisako, J. Magn. Magn. Mater. 320 (2008) 1167–1172.  
 [30] S. Choopani, N. Keyhan, A. Ghasemi, A. Sharbati, R.S. Alam, Mater. Chem. Phys. 113 (2009) 717–720.  
 [31] X. Tang, Y. Yang, K. Hu, J. Alloys Compd. (2008), doi:10.1016/j.jallcom.2008.10.052.  
 [32] L. Zhang, Z. Li, J. Alloys Compd. (2008), doi:10.1016/j.jallcom.2008.01.152.  
 [33] J. Xie, M. Han, L. Chen, R. Kuang, L. Deng, J. Magn. Magn. Mater. 314 (2007) 37–42.  
 [34] T. Nakamura, T. Miyamoto, Y. Yamada, J. Magn. Magn. Mater. 256 (2003) 340–344.  
 [35] A.K. Singh, T.C. Goel, R.G. Mendiratta, O.P. Thakur, C. Prakash, J. Appl. Phys. 91 (2002) 6626–6629.  
 [36] A. Grusková, J. Sláma, R. Dosoudil, M. Ušáková, V. Jančík, E. Ušák, J. Magn. Magn. Mater. 320 (2008) e860–e864.  
 [37] A.R. Bueno, M.L. Gregori, M.C.S. Nóbrega, J. Magn. Magn. Mater. 320 (2008) 864–870.  
 [38] U.R. Lima, M.C. Nasar, R.S. Nasar, M.C. Rezende, J.H. Araújo, J.F. Oliveira, Mater. Sci. Eng. B 151 (2008) 238–242.  
 [39] S.B. Cho, D.H. Kang, J.H. Oh, J. Mater. Sci. 31 (1996) 4719–4722.  
 [40] G.J. Yin, S.B. Liao, IEEE Trans. Magn. 27 (1991) 5459–5461.  
 [41] O.F. Caltun, L. Spinu, A. Sstancu, IEEE Trans. Magn. 37 (2001) 2353–2355.  
 [42] U.R. Lima, M.C. Nasar, R.S. Nasar, M.C. Rezende, J.H. Araújo, J. Magn. Magn. Mater. 320 (2008) 1666–1670.  
 [43] D.C. Kulkarni, S.P. Patil, V. Puri, Microelectron. J. 39 (2008) 248–252.  
 [44] I.H. Gul, A. Maqsood, J. Alloys Compd. 465 (2008) 227–231.  
 [45] J.B. Birks, Progress in Dielectrics, vol. 3, London Heywood & Company Ltd., 1961, p. 153.  
 [46] K.Y. Kim, W.S. Kim, S.Y. Hong, IEEE Trans. Magn. 29 (1993) 2134–2138.